

A FULL BEAM 1D SIMULATION CODE FOR MODELING HYBRID HGHG/EEHG SEEDING SCHEMES FOR EVALUATING THE DEPENDENCE OF BUNCHING FACTOR BANDWIDTH ON MULTIPLE PARAMETERS*

C. Fortgang[#], B. Carlsten, Q. Marksteiner, N. Yampolsky, LANL, Los Alamos, NM USA

Abstract

Multiple seeding schemes are available for design of narrow-band, short-wavelength FELs. Analysis of such schemes often focus on the amplitude of the final bunching factor, b , and how far it is above shot noise. Only under ideal conditions is the bandwidth of b Fourier transform limited. We have developed a 1D simulation tool that models complex hybrid seeding schemes using macro properties of the entire beam bunch to assess effects on both the amplitude and bandwidth of b . In particular the effects on bunching factor from using non-ideal beam driven radiators for downstream modulators, energy slew and curvature, and energy spread are investigated with the 1D tool.

INTRODUCTION

High gain harmonic-generation (HGHG) and echo-enabled harmonic generation (EEHG) as seeding schemes for narrowband short-wavelength FELs is an area of active interest. Much of the published analytical work addresses calculating and maximizing the bunching factor considering a single slice of the beam. However, a single slice calculation of b is not sufficient to estimate the bunching factor bandwidth. Producing a nearly Fourier transformed (FT) limited bunched beam is the primary purpose of seeding so having a prediction of $b(k)$ with realistic beam-bunch macro properties is important. In the case of Ref [1] the spectral width of $b(k)$ is estimated analytically and with simulations but only for the case where the laser pulse is short compared to the electron beam bunch. The work presented here uses the entire beam bunch so the results can be directly compared to an ideal FT limited bunching factor.

1D MODEL BENCHMARKING

The 1D equations for modelling HGHG/EEHG schemes has been discussed in numerous publications [2-4]. Our 1D model includes the FEL physics of modulators and radiators as well as the effects of macro beam properties such as; energy chirp or curvature across the entire beam pulse and a Gaussian current profile $J(z)$ which directly impacts the power profile of a radiator. The effects of phase jitter or chirp across the bunch from a non-ideal external laser are also included.

*Work supported by Laboratory Directed Research and Development at LANL (20110067).
[#]cfortgang@lanl.gov

The following equations are derived from 1D FEL theory [5]. A modulator has to satisfy the condition that $4\pi N_{\text{mod}} \eta \ll 1$ where N_{mod} is the number of modulator periods and $\eta = \Delta\gamma/\gamma$ is the amplitude of the energy modulation. Under this condition electrons are modulated in energy but not in phase.

The amount of laser power required for a desired energy modulation is given by,

$$P_{\text{mod}} = \eta^2 \gamma^4 \sigma_L^2 P_0 / (K_{\text{mod}}^2 [JJ]^2 L_{\text{mod}}^2) \quad \text{where,}$$

σ_L is the laser rms radius and $P_0 = I_{\text{Alfvén}} mc^2/e = 8.7 \text{ GW}$.

Some schemes may use a pre-bunched beam to drive a radiator as a source of laser seed power for a subsequent modulator. The power generated by a radiator is given by,

$$P_{\text{rad}}(z) = Z_0 K_{\text{rad}}^2 [JJ]^2 I_{\text{beam}}^2(z) |b(z)|^2 L_{\text{rad}}^2 / (32\pi \sigma_b^2 \gamma^2)$$

where, $Z_0 = 377 \text{ ohms}$, I_{beam} is the beam current along the bunch, $b(z)$ is the bunching factor along the bunch, and σ_b is the rms electron beam radius. In our 1D model where a radiator is used to drive a modulator the relationship between the electron beam size and the laser transverse power profile is given by $\sigma_L^2 = \sigma_b^2/2$.

The peak amplitudes of the bunching factor harmonics from a HGHG stage is given by [4],

$$b_h = J_h(-h k_{\text{seed}} R_{56} \eta) \exp(-h k_{\text{seed}} R_{56} \sigma_E^2/2)$$

where h is the harmonic number, R_{56} is the HGHG chicane strength, and σ_E is the intrinsic rms energy spread. None of the above equations are used explicitly in the 1D code but rather are used to verify the code results where applicable.

An EEHG stage uses the analytic analysis as outlined in [6]. Using the notation of [6] the important EEHG parameters are $A_1 = \Delta W_1/\sigma_E$, $A_2 = \Delta W_2/\sigma_E$, and $B1 = R1_{56} k_{\text{seed}} \sigma_E/W_0$ and $B2 = R2_{56} k_{\text{seed}} \sigma_E/W_0$ where $A1$ and $A2$ are the normalized energy modulations for the 1st and 2nd energy modulators and $B1$ and $B2$ are the normalized strengths for the strong (1st) and weak (2nd) EEHG chicanes. In the case of a scheme where an EEHG section follows a HGHG section then $B1 = B1^* - B0$ where $B1^*$ would be the strong chicane strength if the HGHG section were absent and $B0$ is the strength of the HGHG chicane.

Determining the ratio of bunching factor to shot noise is an important aspect of seeding analysis. Our 1D code runs fast (a few minutes) using typically 40-80 million macroparticles. For bunch charges in the range of 100-300 pC that implies that the charge/macroparticle is on the order of 20e. The noise in the simulation scales as $N_{\text{macro}}^{-1/2}$ so the code overestimates the shot noise by a factor of ~ 4.5 . When looking at the ratio of $b_{\text{peak}}/(\text{shot noise floor})$ the user needs to take this into account. A good design will have $b \gg \text{shot noise}$ so that the BW of $b(k)$ when defined in one of the usual ways (e.g. 3dB or 10 dB points of $\Delta k/k$) will be determined more by the spectral width (shape) rather than the shot noise floor. Nevertheless the code does satisfy Poisson statistics for the number of macro particles in the simulation. Results for the bunching factor are presented both for the entire bunch and individual slices along the bunch.

NGLS EXAMPLE

To illustrate the utility of our 1D code we consider the NGLS seeding design [7] and some possible variants. The beam parameters as specified in [7] are: $Q=300$ pC, $W=1.8$ GeV, $\sigma_E = 50$ keV, and $I_{\text{peak}} = 500$ A (inferred from $\Delta z_{\text{rms}} = 71.7$ μm). The NGLS scheme is pure EEHG with $\lambda_{\text{seed1}} = \lambda_{\text{seed2}} = 200$ nm, $A1=3.3$, $A2=6.6$, $B1=13.2$, $B2=0.155$ and $\lambda_{\text{echo}} = 2.44$ nm (harmonic=82). The left

hand side of Fig. 1 shows longitudinal phase space and current profiles for a single slice at the center of the bunch for the given NGLS parameters. The right hand side are the same plots but for the values of $A1$ and $A2$ swapped and for $B1=27$ and $B2=0.32$ as dictated by the EEHG design procedure.

The 2 cases have similar bunching factors (shown below) but with qualitatively different phase space and current profiles. As pointed out in [7] the case on the right requires a stronger chicane and thus is more susceptible to CSR effects. However the case on the right has a more constant bunched current profile and thus will be less affected by slippage. Part of our future work is to determine which of these cases has the shorter gain length in the final undulator. The LHS of Fig. 1 agrees very well with Fig. 2 of [7]. Figure 2 shows the bunching factor spectra for the same 2 cases. The top plots are the spectra on a log scale so that the shot noise floor is visible. As discussed above this floor is high by a factor of $((Q/e)/N_{\text{macro}})^{1/2}$. The middle plots are the spectra on a linear scale with the x-axis in terms of harmonic number. The bottom plots zoom in on the peak at k_{echo} . This is the plot that is used to quote a bandwidth for $b(k)$. The bottom plots of Fig. 2 are possible because the entire bunch is modelled.

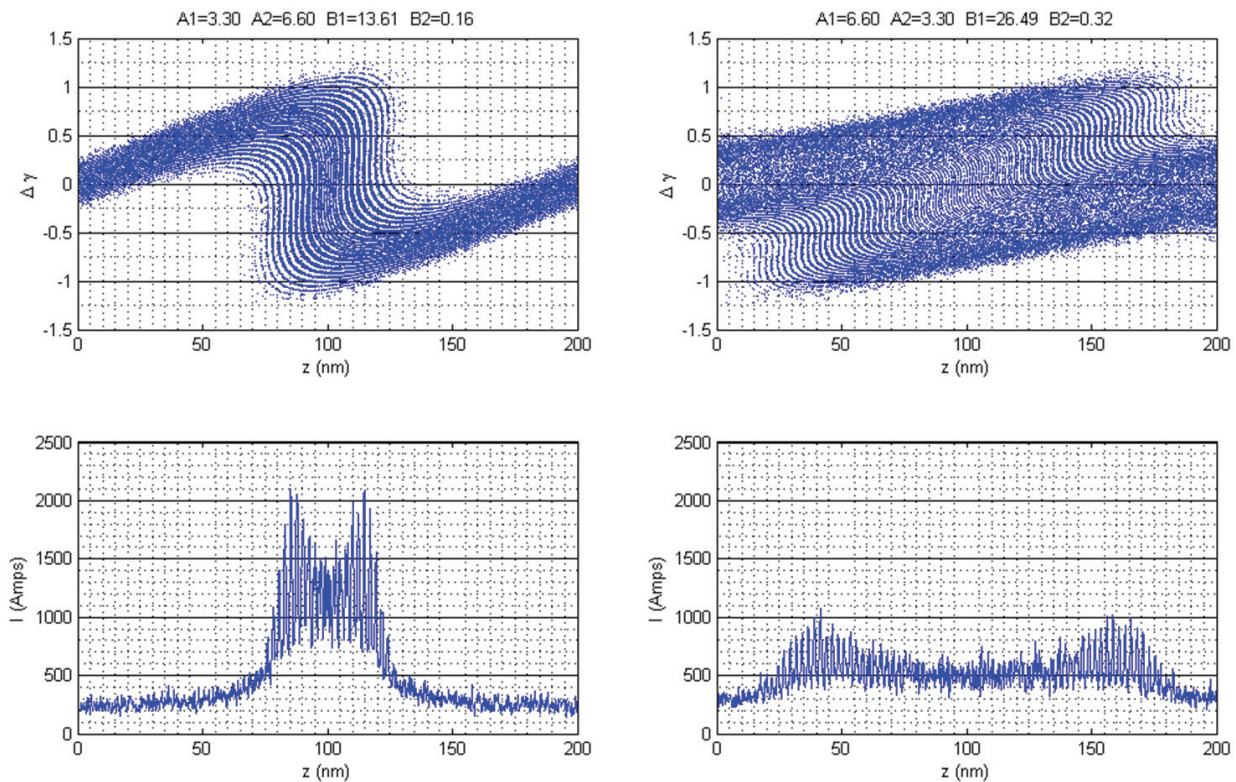


Figure 1: Longitudinal phase space (top) and slice current profiles (bottom) for NGLS design (LHS) and for the case with $A1$ and $A2$ values swapped, with corresponding adjustments to $B1$ and $B2$ (RHS).

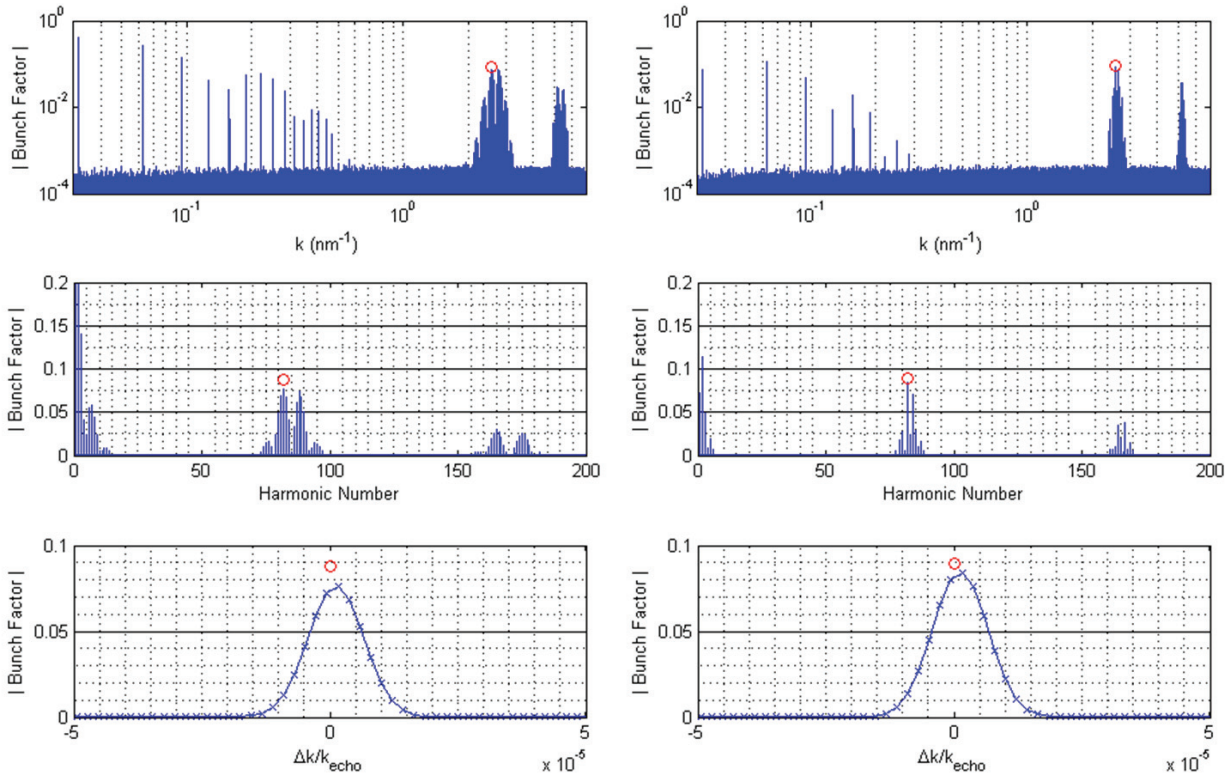


Figure 2: Same 2 cases as Fig. 1. Top is $b(k)$ on a log plot to illustrate the shot noise floor. Middle is the spectra on a linear plot as a function of harmonic number. Bottom plot zooms in on k_{echo} to evaluate the bandwidth at $b(k_{\text{echo}})$. The red circle is the analytic computation of the amplitude of b at k_{echo} [6].

The bandwidth for both cases is $1.5E-5$ whereas the FT limit is estimated to be $(2.355 \Delta z_{\text{rms}} / \lambda_{\text{echo}})^{-1} = 1.45E-5$. It is not surprising that the simulation yields the FT limited bandwidth since there are no non-ideal macro bunch parameters included in this simulation which would affect either the phase or amplitude of $b(z)$.

We conclude this section with a look at the effects of energy curvature across the bunch. The FWHM bunch length out of the NGLS injector is 5 ps, accelerated with 1.3 GHz RF to 350 MeV [8], where it is compressed to $\Delta z_{\text{rms}} = 71.7 \mu\text{m}$. Assuming a worst case where the bunch rides on the crest of the RF these numbers correspond to an energy curvature across the bunch at $z = \pm \text{FWHM}/2$ of $\Delta W = -73 \text{ keV}$ or 1.5 times the intrinsic energy spread. With $A1=3.3$ this amount of energy curvature has an effect on b but not a large one. To exaggerate the effect for the 1D simulation results we double the energy curvature to 146 keV. Figure 3 shows the effect of the energy curvature on both the amplitude and phase of $b(z)$ across the bunch. There is no effect on $|b(z)|$ but the curvature does induce a quadratic phase shift of b along the bunch.

Figure 4 shows $b(k)$ for the entire bunch for NGLS parameters and with the energy curvature effect included. This result should be compared to the LHS of Fig. 2.

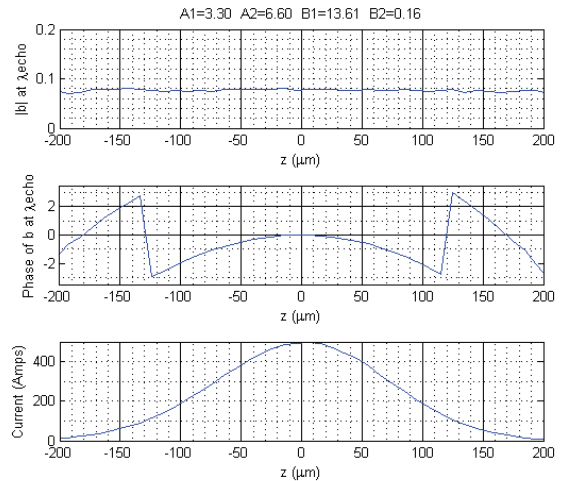


Figure 3: The effect of energy curvature on the bunching factor magnitude and phase as a function of length along the bunch. The effect is seen as a quadratic phase shift.

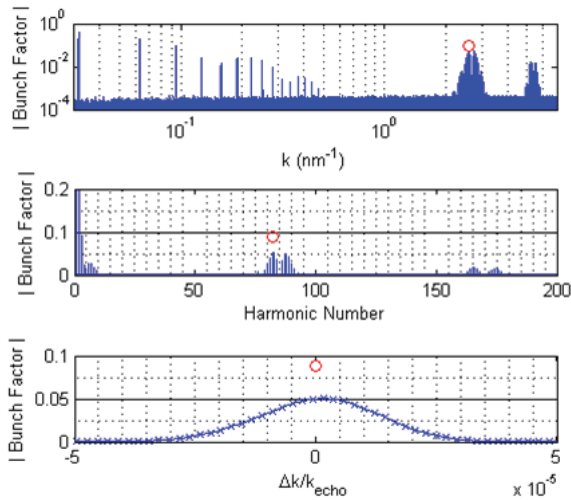


Figure 4: Bunching factor spectra for the NGLS parameters with energy curvature included. The $|b|$ decreases and the bandwidth at k_{echo} increases.

Because of the quadratic phase chirp across the bunch the bunching factor at k_{echo} decreases by 33% and the bandwidth increases by a factor of 2 to $3E-5$.

The 1D code also includes effects (e.g. phase noise and/or chirp) from a non-ideal external laser but those results are not included here. This topic has been addressed with simulations elsewhere [1] and we observe similar effects, particularly to the phase of the bunching factor and the resultant increase in bandwidth.

A HYBRID HGHG/EEHG EXAMPLE

Figure 5 shows the architecture of a hybrid HGHG/EEHG scheme. The idea here is to use a HGHG section followed by a radiator as the laser source for the subsequent EEHG section. With this scheme a 40 nm

radiator replaces the 2nd 200 nm external laser used in the pure EEHG architecture. We keep λ_{echo} at 2.44 nm. The 40 nm radiator parameters are: $K=2.99$, period=18.2 cm and $N_{\text{rad}}=20$. The 40 nm modulator parameters are: $K=0.84$, period=73.4 cm, and $N_{\text{mod}}=5$. With these parameters the modulator requires, and the radiator produces at the bunch center, about 11.3 MW. Note that for this architecture $A1>A2$, the opposite of the NGLS approach where $A2>A1$ results in a weaker first chicane in the EEHG section. However, with the shorter wavelength laser provided by the radiator (40 nm vs. 200 nm) the strength of the strong chicane is greatly reduced so the downside of having $A1>A2$ is no longer present. An obvious drawback of using a radiator is that the power profile along the radiation pulse scales as $I_{\text{beam}}^2(z)$. This implies that with lower than required laser power off peak the energy modulation is less than desired. We now investigate this effect on the bunching factor. Figure 6 shows the magnitude and phase of $b(k_{\text{echo}})$ along the bunch, and the Gaussian current profile. Note that in the core of the bunch both the amplitude and phase of the bunching factor is approximately constant. Outside the core the amplitude quickly falls off and the phase becomes random, a consequence of the lower than necessary laser power for the EEHG modulator. However, it is interesting to note that with this hybrid scheme the magnitude of b at the center of the bunch is 0.12, higher than the 0.075 value obtained with the NGLS pure EEHG architecture of the previous section (Fig. 2). This is a consequence of lowering the harmonic number in the EEHG section by decreasing the wavelength of the laser used in the EEHG modulator.

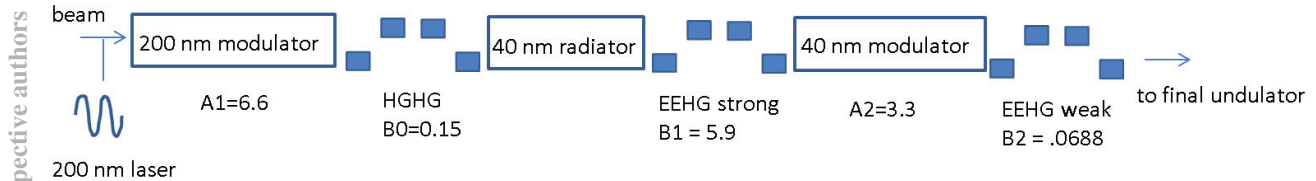


Figure 5: Layout of a hybrid HGHG/EEHG architecture with parameters for the given example.

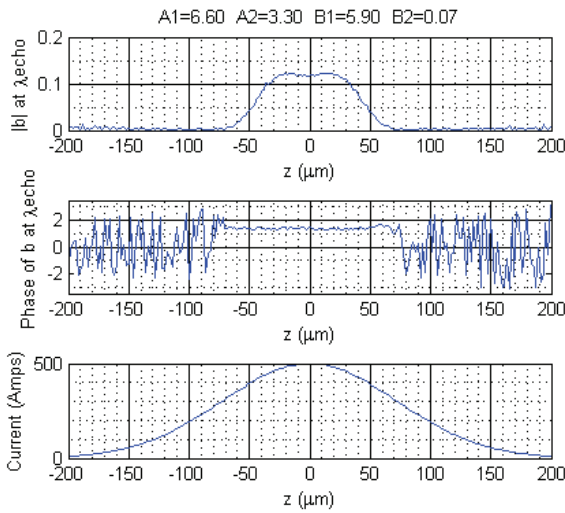


Figure 6: Amplitude and phase of $b(k_{\text{echo}})$ along the bunch for the hybrid HGHG/EEHG scheme. Bottom plot is the bunch current profile.

Though the amplitude of b is higher in the core of the bunch we expect, when averaged over the entire bunch, $|b|$ to decrease and the bandwidth to increase because of the shorter effective length of coherent bunching. As shown in Fig. 7, indeed this is the case. The amplitude of b has dropped to 0.055 from 0.075 and the bandwidth has increased to $3.E-5$ from the previously obtained FT limited case of $1.5E-5$.

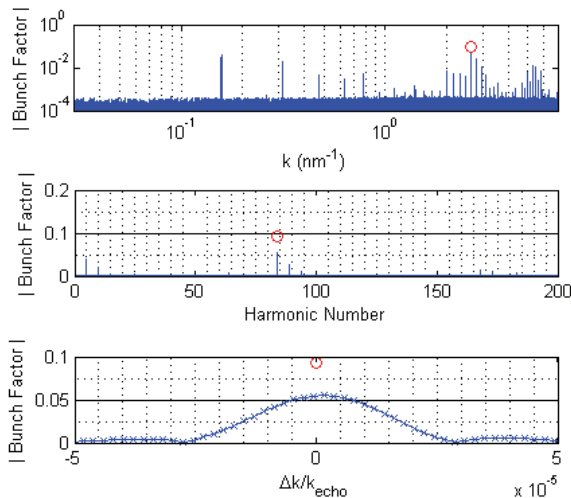


Figure 7: Bunching factor spectra for the hybrid HGHG/EEHG architecture. The amplitude of $b(k_{\text{echo}})$ decreases and the bandwidth increases when b is calculated using the entire bunch.

For this same hybrid case Fig. 8 shows longitudinal phase space at the center of the bunch as the beam exits the 40 nm radiator. The energy is modulated at 200 nm and 40 nm. There is no additional bunching on the beam due to the radiator.

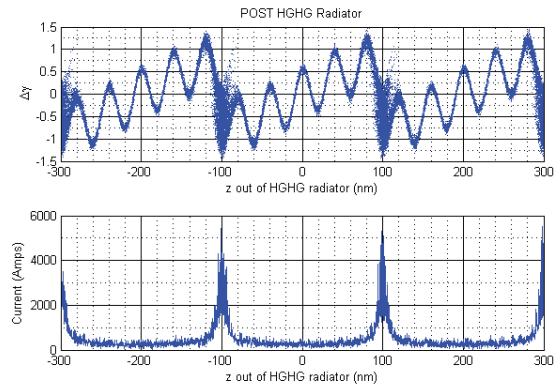


Figure 8: Longitudinal phase space after the HGHG radiator calculated using the embedded 1D FEL code. Note the 200 nm and 40 nm energy modulation. The current is modulated at 200 nm but not at 40 nm.

SUMMARY

Examples of simulations from a 1D seeding code that takes into account effects that are seen only when the entire bunch length is considered has been presented. By modelling the entire bunch one can investigate the bunching parameter bandwidth, this cannot be done with a single slice calculation or simulation. The code allows the user to investigate the effects of macro properties across the bunch such as energy chirp, energy curvature; and non-constant laser power and phase from either external lasers or radiators. The 1D FEL equations are embedded in the code so it more realistically models radiators. Therefore the effect of the radiation back on the beam is included as well as the effect of using that non-ideal radiation in a follow-on modulator. The code is flexible enough so that fairly complicated seeding schemes can be assessed for both amplitude and bandwidth of the bunching factor.

REFERENCES

- [1] D. Ratner et al., Phys. Rev. ST Accel. Beams 15, 030702 (2012).
- [2] L.H. Yu, Phys. Rev. A 44 (1991) 5178.
- [3] L.H. Yu and J.H. Wu, Nucl. Inst. Methods Phys. Rev. A, 483 (2002) 493.
- [4] Z. Huang, “An Analysis of Shot Noise Propagation and Amplification in Harmonic Cascade FELs”, FEL Conference, Berlin, 2006, MOPPH042.
- [5] Z. Huang, US Part. Accel. School, 2013, unpublished
- [6] D. Xiang and G. Stupakov, Phys. Rev. ST Accel. Beams 12 (2009) 030702.
- [7] G. Penn and M. Reinsch, J. Mod. Opt. 58 (2011) 1404.
- [8] LBNL CD-0 Proposal, “A Next Generation Light Source”, Dec. 2010.